

AN INTERPOLATED GALERKIN FINITE ELEMENT METHOD FOR THE POISSON EQUATION

TATYANA SOROKINA¹ AND SHANGYOU ZHANG

ABSTRACT. When solving the Poisson equation by the finite element method, we use one degree of freedom for interpolation by the given Laplacian – the right hand side function in the partial differential equation. The finite element solution is the Galerkin projection in a smaller vector space. The idea is similar to that of interpolating the boundary condition in the standard finite element method. Due to the pointwise interpolation, our method yields a smaller system of equations and a better condition number. The number of unknowns on each element is reduced significantly from $(k^2 + 3k + 2)/2$ to $3k$ for the P_k ($k \geq 3$) finite element. We construct 2D P_2 conforming and nonconforming, and P_k ($k \geq 3$) conforming interpolated Galerkin finite elements on triangular grids. This interpolated Galerkin finite element method is proved to converge at the optimal order. Numerical tests and comparisons with the standard finite elements are presented, verifying the theory and showing advantages of the interpolated Galerkin finite element method.

Keywords: finite element, interpolated finite element, triangular grid, Poisson equation.

AMS subject classifications. 65N30, 65N15.

1. INTRODUCTION

Standard finite element methods use the full P_k polynomials (of total degree $\leq k$) on each element (e.g. triangle or tetrahedron), in order to achieve the optimal order of approximation, in solving partial differential equations. In certain situations the P_k polynomial space is enriched by the so-called bubble functions, for stability or continuity, cf. [2, 4, 5, 6, 7, 8, 9, 12, 18, 19, 20, 22]. But only in one case we use a proper subspace of P_k polynomials while retaining the optimal order, $O(h^k)$ in H^1 -norm, of convergence. That is the harmonic finite element method for solving the Laplace equation, $\Delta p = p_{xx} + p_{yy} = 0$, where only harmonic polynomials in P_k are used [14, 15].

For example, in the P_2 nonconforming element method for solving the following Laplace equation,

$$\begin{aligned} -\Delta u &= 0, & \text{in } \Omega, \\ u &= f, & \text{on } \partial\Omega, \end{aligned} \tag{1.1}$$

where Ω is a bounded polygonal domain in \mathbb{R}^2 , the five basis functions on the element boundary are harmonic polynomials and only the sixth basis function (which

¹ The author is partially supported by the grant from the Simons Foundation #235411 to Tatyana Sorokina.

vanishes on the 6 Gauss-Legendre points on the three edges) is not a harmonic polynomial. So, in [15], the 6th basis function of the P_2 nonconforming element is thrown away, on every triangle, in the harmonic finite element method. For example, on a uniform triangular grid on a square domain, the number of unknowns is reduced from $(2n - 1)^2 + 2n^2$ to $(2n - 1)^2$, about one-third less. But the harmonic finite element method cannot be applied directly to the Poisson equation,

$$\begin{aligned} -\Delta u &= f, & \text{in } \Omega, \\ u &= 0, & \text{on } \partial\Omega, \end{aligned} \tag{1.2}$$

where Ω is a bounded polygonal domain in \mathbb{R}^2 . The sixth basis function of P_2 nonconforming finite element must be added to the harmonic finite element method. This is then the standard P_2 nonconforming element method where the solution is

$$u_h = \sum_{\mathbf{x}_i \in \partial K \setminus \partial\Omega} u_i \phi_i + \sum_{\mathbf{x}_j \in K^\circ} u_j \phi_j + \sum_{\mathbf{x}_k \in \partial\Omega} c_k \phi_k, \tag{1.3}$$

where c_k are interpolated values on the boundary, and u_i and u_j are obtained from the Galerkin projection (from the solution of a discrete linear system of equations). But the sixth basis function is local and the only non-harmonic polynomial which can be obtained from the right hand side function f in (1.2). That is, the solution of the P_2 nonconforming interpolated Galerkin finite element is

$$u_h = \sum_{\mathbf{x}_i \in \partial K \setminus \partial\Omega} u_i \phi_i + \sum_{\mathbf{x}_j \in K^\circ} c_j \phi_j + \sum_{\mathbf{x}_k \in \partial\Omega} c_k \phi_k, \tag{1.4}$$

where c_j (could be $f(\mathbf{x}_j)$ depending on which ϕ_j is used) are interpolated values of the right hand side function f , c_k are interpolated boundary values, and only u_i are obtained from the Galerkin projection. The new method does not only reduce the number of unknowns (from $O(k^2)$ to $O(k)$), but also improves the condition number. It is totally different from the traditional finite element static condensation which does Gaussian elimination from internal degrees of freedom first.

In this work, in addition to constructing special P_2 conforming and nonconforming interpolated finite elements, we redefine the basis functions of the P_k ($k \geq 3$) Lagrange finite element. We keep the Lagrange nodal values on the boundary of each element, and replace the internal Lagrange nodal values by the internal Laplacian values at these internal Lagrange nodes. This way, the linear system of Galerkin projection equations involves only the unknowns on the inter-element boundary. Therefore the number of unknowns on each element is reduced from $(k + 1)(k + 2)/2$ to $3k$ as all internal unknowns are interpolated by the given function f directly. We show that the interpolated Galerkin finite element solution converges at the optimal order. Numerical tests are provided to the above mentioned interpolated Galerkin finite elements, in comparison with the standard finite element method.

2. THE P_2 INTERPOLATED GALERKIN CONFORMING FINITE ELEMENT

The P_2 interpolated Galerkin conforming finite element is defined only on macro-element grids, while the rest higher order P_k elements are defined on general triangular grids. We will define another P_2 interpolated nonconforming element next section on general triangular grids.

A P_2 harmonic polynomial is a linear combination of $1, x, y, x^2 - y^2$ and xy . A P_2 interpolated finite element basis function is a linear combination of $1, x, y, x^2 - y^2, xy$ and $x^2 + y^2$. Only the last basis function has a non-zero Laplacian.

Let the union of four triangles $\hat{K} = \cup_{i=1}^4 K_i$ be a reference macro-element shown in Figure 2.1 (left). On the reference macro-element \hat{K} , the P_2 finite element space is

$$P_{\hat{K}} := \{v_h \in L^2(\hat{K}) \mid v_h|_{K_i} \in P_2; v_h \in C^0(\mathbf{x}_i), i = 1, 2, 3, 4; \quad (2.1) \\ v_h \in C^1(\mathbf{x}_9); \Delta v_h \in P_0\},$$

where $v_h \in C^0(\mathbf{x}_i)$ means that the two adjoining at \mathbf{x}_i polynomial pieces of v_h have the same value at \mathbf{x}_i , $v_h \in C^1(\mathbf{x}_9)$ means that the four adjoining at \mathbf{x}_9 polynomial pieces of v_h and its first derivatives have matching values at \mathbf{x}_9 , and $\Delta v_h \in P_0$ means that the four adjoining at \mathbf{x}_9 polynomial pieces of v_h have a matching constant Laplacian. These conditions immediately imply that v_h is continuous on \hat{K} . We will show that the dimension of the space $P_{\hat{K}}$ is 9, and each such P_2 function is uniquely determined by its 8 nodal values, $v_h(\mathbf{x}_i)$, $i = 1, 2, \dots, 8$, and the value of Δv_h , see Figure 2.1 (left).

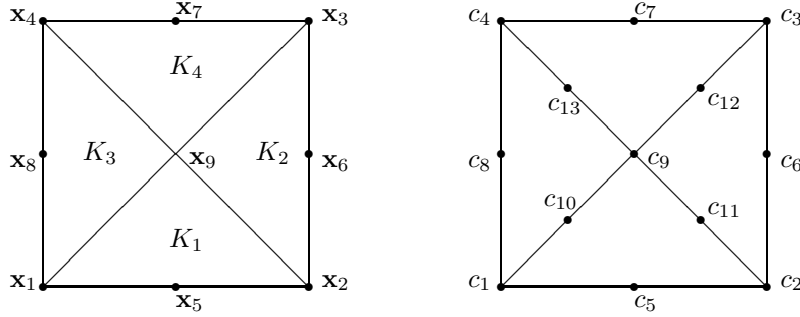


FIGURE 2.1. The reference macro-element, $\hat{K} = \cup_{i=1}^4 K_i = [-1, 1]^2$ (left), and the B-coefficients associated with the domain points in \hat{K} (right)

Theorem 2.1. Consider $S_2^0(\hat{K}) \xrightarrow{\Delta} S_0^{-1}(\hat{K})$, where

$$S_2^{0,1}(\hat{K}) := \{s|_{K_i} \in P_2, i = 1, 2, 3, 4; s \in C^1(\mathbf{x}_9); s \in C^0(\hat{K})\}, \\ S_0^{-1}(\hat{K}) := \{s|_{K_i} \equiv c_i \in \mathbb{R}, i = 1, 2, 3, 4\}.$$

Then the image of $S_2^0(\hat{K})$ is a three dimensional subspace of $S_0^{-1}(\hat{K})$ consisting of piecewise constants satisfying the condition $c_1 - c_2 + c_3 - c_4 = 0$.

Lemma 2.1. The conforming P_2 finite element function $u_h \in P_{\hat{K}_h}$ is unisolvent by the eight nodal values, $u_h(\mathbf{x}_i)$, $i = 1, 2, \dots, 8$, and the value $\Delta u_h(\mathbf{x}_9)$.

Proof. We use the Bernstein-Bézier form of u_h on \hat{K}_h with the B-coefficients c_1, c_2, \dots, c_{13} associated with the domain points in \hat{K}_h as depicted in Figure 2.1 (right), see e.g. Chapter 2 of [10] for relevant definitions. Using the eight nodal values, $u_h(\mathbf{x}_i)$, $i = 1, 2, \dots, 8$, we compute the eight B-coefficients by interpolation

conditions as follows

$$\begin{aligned} c_i &= u_h(\mathbf{x}_i), & i &= 1, \dots, 4, \\ c_5 &= 2u_h(\mathbf{x}_5) - (c_1 + c_2)/2, & c_6 &= 2u_h(\mathbf{x}_6) - (c_2 + c_3)/2, \\ c_7 &= 2u_h(\mathbf{x}_7) - (c_3 + c_4)/2, & c_8 &= 2u_h(\mathbf{x}_8) - (c_4 + c_1)/2. \end{aligned}$$

By Lemma 4.1 in [1], the following four conditions are necessary and sufficient for $\Delta u_h = \Delta u_h(\mathbf{x}_9)$ on each triangle K_i , $i = 1, \dots, 4$, in the square \hat{K}_h :

$$\begin{aligned} 2c_9 + c_1 + c_2 - 2c_{10} - 2c_{11} &= \Delta u_h(\mathbf{x}_9)/2, \\ 2c_9 + c_2 + c_3 - 2c_{11} - 2c_{12} &= \Delta u_h(\mathbf{x}_9)/2, \\ 2c_9 + c_3 + c_4 - 2c_{12} - 2c_{13} &= \Delta u_h(\mathbf{x}_9)/2, \\ 2c_9 + c_4 + c_1 - 2c_{13} - 2c_{10} &= \Delta u_h(\mathbf{x}_9)/2. \end{aligned} \tag{2.2}$$

By Theorem 2.28 in [10], the following two conditions are necessary and sufficient for u_h to be C^1 at the center \mathbf{x}_9 of the square \hat{K}_h :

$$\begin{aligned} 2c_9 - c_{10} - c_{12} &= 0, \\ 2c_9 - c_{11} - c_{13} &= 0. \end{aligned} \tag{2.3}$$

Note that the alternating sum of the four equations in (2.2) vanishes. Thus we only consider the first three equations of (2.2). Substituting $c_{13} = c_{10} + c_{12} - c_{11}$, and $2c_9 = c_{10} + c_{12}$ from (2.3), into (2.2), we obtain a system of three equations with three unknowns that has a unique solution given by

$$\begin{aligned} c_9 &= (c_1 + c_2 + c_3 + c_4 - 2\Delta u_h(\mathbf{x}_9))/4, \\ c_{10} &= (2c_1 + c_2 + c_4 - \Delta u_h(\mathbf{x}_9))/4, \\ c_{11} &= (2c_2 + c_1 + c_3 - \Delta u_h(\mathbf{x}_9))/4, \\ c_{12} &= (2c_3 + c_2 + c_4 - \Delta u_h(\mathbf{x}_9))/4, \\ c_{13} &= (2c_4 + c_1 + c_3 - \Delta u_h(\mathbf{x}_9))/4. \end{aligned} \tag{2.4}$$

Therefore, all thirteen B-coefficients c_1, c_2, \dots, c_{13} have been uniquely determined by the eight nodal values $u_h(\mathbf{x}_i)$, $i = 1, 2, \dots, 8$, and by $\Delta u_h(\mathbf{x}_9)$. \blacksquare

Let $\mathcal{M}_h = \{K : \cup K = \Omega\}$ be a square subdivision of the domain Ω . We subdivide each rectangle K into four triangles K_i as in Figure 2.1, and let $\mathcal{T}_h = \{K_i : K_i \subset K\}$ be the corresponding triangular grid of grid-size h . The P_2 finite element space on the grid is defined by

$$V_h = \{v_h \in H_0^1(\Omega) \mid v_h|_K = \sum_{i=1}^8 c_i \phi_i + c_9 \phi_9 \in P_K \ \forall K \in \mathcal{M}_h\}, \tag{2.5}$$

where P_K is defined in (2.1), basis $\phi_i(\mathbf{x}_j) = \delta_{ij}$ and $\Delta \phi_{i9}(\mathbf{x}_9) = \delta_{i9}$. The interpolated Galerkin finite element problem reads: Find $u_h = \sum_{K \in \mathcal{M}_h} \left(\sum_{i=1}^8 u_i \phi_i - f(\mathbf{x}_9) \phi_9 \right)$ such that

$$(\nabla u_h, \nabla v_h) = (f, v_h) \quad \forall v_h = \sum_{K \in \mathcal{M}_h} \sum_{i=1}^8 v_i \phi_i. \tag{2.6}$$

3. THE P_2 INTERPOLATED NONCONFORMING FINITE ELEMENT

We define a P_2 interpolated Galerkin nonconforming finite element on general triangular grids in this section. This element is the best one to describe the difference between interpolated Galerkin finite element methods and standard Galerkin finite element methods. The P_2 nonconforming finite element function is continuous on the two Gauss-Legendre points of every edge. But the set of 6 nodal values of a 6-dimensional P_2 polynomial is linearly dependent. We can use the 5-dimensional harmonic P_2 polynomials to build these 5 basis functions which has non-zero values at the 6 Gauss-Legendre points and zero Laplacian at the barycenter of triangle. As these 6 Gauss-Legendre points on edges are always on an ellipse, the last P_2 basis function has a constant Laplacian 1 everywhere on the triangle and vanishes at the Gauss-Legendre points. This is how the basis functions are defined in the standard P_2 nonconforming finite element. Now, instead of solving the coefficient of this last basis function from the discrete equations, we can interpolate the right hand side function to get this coefficient directly.

Let \mathcal{T}_h be a shape-regular, quasi-uniform triangulation on Ω . The P_2 nonconforming interpolated finite element space is defined by

$$\begin{aligned}
 V_h = \{v_h \in L^2(\Omega) \mid & v_h \text{ is continuous at two Gauss points each edge ,} \\
 & v_h \text{ is zero at two Gauss points on boundary edge ,} \\
 & v_h|_K = \sum_{i=1}^5 c_i \phi_i + c_0 \phi_0 \in P_2(K) \forall K \in \mathcal{T}_h\}, \tag{3.1}
 \end{aligned}$$

where $\{\phi_i, i = 1, \dots, 5\}$ are global basis functions restricted on K which are P_2 harmonic functions (i.e., spanned by $\{1, x, y, xy, x^2 - y^2\}$, cf. [15]) and $\Delta\phi_0(\mathbf{x}_0) = -1$, $\phi_0(\mathbf{x}_i) = 0$, $i = 1, \dots, 5$, cf. Figure 3.1.

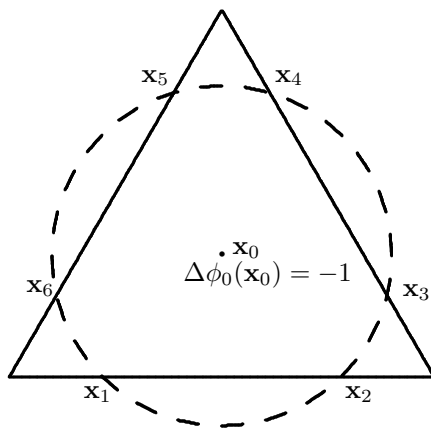


FIGURE 3.1. Nodal points of P_2 non-conforming finite elements.

The P_2 -nonconforming, interpolated Galerkin finite element problem reads: Find $u_h = \sum_{K \in \mathcal{T}_h} \left(\sum_{i=1}^5 u_i \phi_i + f(\mathbf{x}_0) \phi_0 \right)$ such that

$$(\nabla_h u_h, \nabla_h v_h) = (f, v_h) \quad \forall v_h = \sum_{K \in \mathcal{T}_h} \sum_{i=1}^5 v_i \phi_i. \quad (3.2)$$

4. P_k ($k \geq 3$) INTERPOLATED GALERKIN FINITE ELEMENTS

There is no P_1 interpolated finite element as the Laplacian of a P_1 polynomial is zero. It needs special cares for P_2 interpolated finite elements, as we did in the last two sections. But for P_3 and above interpolated finite elements, we can simply replace all internal Lagrange degrees of freedom by the Laplacian values, which are obtained from the given right hand side function f . However we could not prove the uni-solvence for general k . We define another type interpolated finite element for P_k ($k \geq 4$), where we use local averaging Laplacian values in stead of pointwise Laplacian value.

Let \mathcal{T}_h be a shape-regular, general quasi-uniform triangulation on Ω . The P_3 interpolated finite element space is defined by

$$V_h = \{v_h \in H_0^1(\Omega) \mid v_h|_K = \sum_{i=1}^9 c_i \phi_i + c_0 \phi_0 \in P_3(K) \forall K \in \mathcal{T}_h\}, \quad (4.1)$$

where $\{\phi_i, i = 1, \dots, 9\}$ are boundary Lagrange basis functions which have vanishing Laplacian at the barycenter \mathbf{x}_0 of K , and ϕ_0 vanishes on the three edges of K and $\Delta \phi_0(\mathbf{x}_0) = -1$, cf. Figure 4.1.

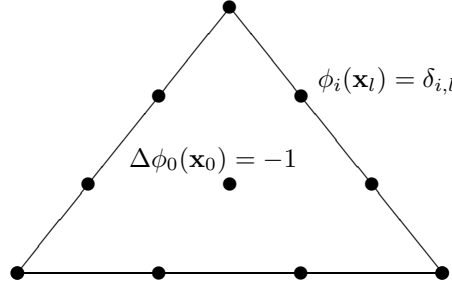


FIGURE 4.1. Nodal points of P_3 interpolated finite elements.

Lemma 4.1. *The $(9 + 1)$ nodal degrees of freedom in (4.1) uniquely define a P_3 polynomial.*

Proof. We have a square system of 9 linear equations with 9 unknowns. The uniqueness guarantees existence. Let u_h be a solution of the homogeneous system. Then u_h vanishes on 3 edges, cf. Figure 4.1. $u_h = Cb$, where b is the P_3 bubble function on K , vanishing on the edges and assuming value 1 at the barycenter \mathbf{x}_0 . Since $\Delta u_h(\mathbf{x}_0) = 0$ and Δu_h is a linear function, we have, by symmetry,

$$\begin{aligned} 0 &= -\Delta u_h(\mathbf{x}_0)b = -\int_K (\Delta u_h)b \, d\mathbf{x} \\ &= \int_K \nabla u_h \cdot \nabla b \, d\mathbf{x} = C \int_K |\nabla b|^2 \, d\mathbf{x}. \end{aligned}$$

Thus $C = 0$, $u_h = 0$ and the lemma is proved. ■

The P_3 interpolated Galerkin finite element problem reads:

$$\begin{aligned} \text{Find } u_h &= \sum_{K \in \mathcal{T}_h} \left(\sum_{i=1}^9 u_i \phi_i + f(\mathbf{x}_0)_K \phi_0 \right) \text{ such that} \\ (\nabla u_h, \nabla v_h) &= (f, v_h) \quad \forall v_h = \sum_{K \in \mathcal{T}_h} \sum_{i=1}^9 v_i \phi_i. \end{aligned} \quad (4.2)$$

For defining P_k ($k \geq 4$) interpolated finite elements, we explicitly define two types degrees of freedom. Let boundary nodal-value linear functional F_i be

$$F_i(u) = u(\mathbf{x}_i), \quad i = 1, \dots, 3k, \quad \text{cf. Figure 4.2.} \quad (4.3)$$

Let the Laplacian moment linear functional G_j be

$$G_j(u) = \int_K p_j b \Delta u \, d\mathbf{x}, \quad j = 1, \dots, d_{k-3}, \quad (4.4)$$

where p is again the cubic bubble function on K , $d_{k-3} = \dim P_{k-3}$, and $\{p_j\}$ is an orthonormal basis obtained by the Gram-Schmidt process on $\{p_j = 1, x, y, x^2, \dots, y^{k-3}\}$ under the inner product

$$(u, v)_G = \int_K \nabla(bu) \cdot \nabla(bv) \, d\mathbf{x}.$$

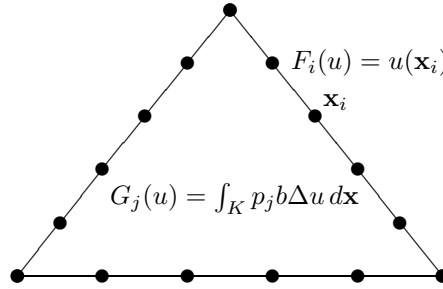


FIGURE 4.2. Nodal points and moments of P_5 interpolated finite elements.

Lemma 4.2. *The $(3k + d_{k-3})$ linear functionals in (4.3) and (4.4) uniquely define a P_k polynomial.*

Proof. Because $\dim P_k = 3k + d_{k-3}$, we have a square linear system of equations when applying the functionals to determine a P_k polynomial. We only need to show the uniqueness.

Let $u \in P_k$ such that $F_i(u) = 0$ and $G_j(u) = 0$, $i = 1, \dots, 3k$, $j = 1, \dots, d_{k-3}$. Because $u = 0$ on the three edges (cf. Figure 4.2) we have

$$u = bp \text{ for some } p \in P_{k-3}.$$

Let the combination of p_j in G_j , defined in (4.4), be p . We get

$$\begin{aligned} 0 &= \sum_{j=0}^{d_k-3} c_j G_j(u) = \int_K \sum_{j=0}^{d_k-3} c_j p_j b \Delta u \, d\mathbf{x} \\ &= \int_K p b \Delta u \, d\mathbf{x} = \int_K |\nabla u|^2 \, d\mathbf{x}. \end{aligned}$$

Thus $\nabla u = 0$ and $u = C$. Because $u = bp = 0$ on the boundary, $u = C = 0$. The proof is completed. \blacksquare

The P_k ($k \geq 4$) interpolated finite element space is defined by

$$V_h = \{v_h \in H_0^1(\Omega) \mid v_h|_K = \sum_{i=1}^{3k} c_i \phi_i + \sum_{j=1}^{d_k-3} c_j \psi_j \in P_k(K) \, \forall K \in \mathcal{T}_h\}, \quad (4.5)$$

where $\{\phi_i, \psi_j\}$ is the dual basis of $\{F_i, G_j\}$, by Lemma 4.2. The P_k ($k \geq 4$) interpolated Galerkin finite element problem reads:

$$\text{Find } u_h = \sum_{K \in \mathcal{T}_h} \left(\sum_{i=1}^{3k} u_i \phi_i - \sum_{j=1}^{d_k-3} (f, \psi_j)_K \psi_j \right) \text{ such that} \quad (4.6)$$

$$(\nabla u_h, \nabla v_h) = (f, v_h) \quad \forall v_h = \sum_{K \in \mathcal{T}_h} \sum_{i=1}^{3k} v_i \phi_i. \quad (4.7)$$

5. CONVERGENCE THEORY

Theorem 5.1. *Let u and u_h be the exact solution of (1.2) and the P_k ($k \geq 4$) interpolated finite element solution of (4.7), respectively. Then*

$$\|u - u_h\|_0 + h|u - u_h|_1 \leq Ch^{k+1}|u|_{k+1}, \quad (5.1)$$

where $|\cdot|_k$ is the Sobolev (semi-)norm $H^k(\Omega)$.

Proof. Testing (1.2) by $v_h = \phi_i \in H_0^1(\Omega)$, we have

$$(\nabla u, \nabla v_h) = (f, v_h). \quad (5.2)$$

Subtracting (4.7) from (5.2),

$$(\nabla(u - u_h), \nabla v_h) = 0. \quad (5.3)$$

Testing (1.2) by $v_h = \psi_j \in H_0^1(\Omega)$, by (4.4) and (4.6), we get

$$\begin{aligned} (\nabla(u - u_h), \nabla \psi_j) &= - \int_K \Delta u \psi_j \, d\mathbf{x} - (f, \psi_j)_K \int_K |\nabla \psi_j|^2 \, d\mathbf{x} \\ &= \int_K f \psi_j \, d\mathbf{x} - (f, \psi_j)_K = 0. \end{aligned} \quad (5.4)$$

Combining (5.3) and (5.4) implies

$$\begin{aligned} |u - u_h|_1^2 &= (\nabla(u - u_h), \nabla(u - I_h u)) \\ &\leq |u - u_h|_1 |u - I_h u|_1 \leq |u - u_h|_1 Ch^k \|u\|_{k+1}, \end{aligned}$$

where I_h is the interpolation operator to V_h . This completes the H^1 estimate. Let $w \in H^2(\Omega) \cap H_0^1(\Omega)$ solve

$$(\nabla w, \nabla v) = (u - u_h, v) \quad \forall v \in V_h.$$

We assume H^2 regularity for the solution, i.e.,

$$\|w\|_2 \leq C\|u - u_h\|_0.$$

Let w_h be P_k interpolated finite solution of w . Then

$$\begin{aligned} \|u - u_h\|_0^2 &= (\nabla w, \nabla(u - u_h)) = (\nabla(w - w_h), \nabla(u - u_h)) \\ &\leq |w - w_h|_1 |u - u_h| \leq Ch|w|_2 Ch^k \|u\|_{k+1} \\ &\leq \|u - u_h\|_0 Ch^{k+1} \|u\|_{k+1}. \end{aligned}$$

This gives the L^2 error estimate. ■

Theorem 5.2. *Let u be the exact solution of (1.2). Let u_h the P_2 conforming, or the P_2 nonconforming, or the P_3 finite element solution of (2.6), (3.2), or (4.2), respectively. Then*

$$\|u - u_h\|_0 + h|u - u_h|_1 \leq Ch^{k+1} |u|_{k+1}, \quad (5.5)$$

where $k = 2$, or 3.

Proof. As there is one local/internal Laplacian degree of freedom, the proof becomes very simple. Testing (1.2) by nodal value basis $\tilde{v}_h = \phi_i$, we have

$$(\nabla u, \nabla \tilde{v}_h) = (f, v_h). \quad (5.6)$$

Subtracting finite element equations from (5.6),

$$(\nabla(u - \tilde{u}_h - u_0), \nabla v_h) = 0,$$

where we separate the finite element solution u_h in to two parts, the nodal basis span part \tilde{u}_h and the interpolated Laplacian part u_0 (spanned by the last basis function ϕ_0 .) Thus

$$\begin{aligned} |u - u_h|_1^2 &= (\nabla(u - \tilde{u}_h - u_0), \nabla(u - \tilde{v}_h - u_0)) \\ &= (\nabla(u - \tilde{u}_h - u_0), \nabla(u - I_h u)) \\ &\leq |u - u_h|_1 |u - I_h u|_1 \leq |u - u_h|_1 Ch^k \|u\|_{k+1}, \end{aligned}$$

where I_h is the interpolation operator to V_h . This completes the H^1 estimate. The L^2 error estimate is identical to above proof for Theorem 5.1. The treatment for the inconsistency by P_2 nonconforming element is standard, cf. [11, 15, 16, 17, 21].

■

6. NUMERICAL TESTS

Let the domain of the boundary value problem (1.2) be $\Omega = (0, 1)^2$. The exact solution is $u(x, y) = \sin \pi x \sin \pi y$. We chose a family of uniform triangular grids, shown in Figure 6.1, in all numerical tests on P_k interpolated Galerkin finite element methods.

We solve problem (1.2) first by the P_2 interpolated Galerkin conforming finite element method defined in (2.6) and by the P_2 Lagrange finite element method, on same grids. The errors and the orders of convergence are listed in Table 6.1. Both elements converge at the optimal order.

Next we solve the test problem (1.2) again, by the P_2 interpolated non-conforming finite element method (3.2) and by the standard P_2 nonconforming finite element method. The errors and the orders of convergence are listed in Table 6.2. Again, both methods converge in the optimal order.

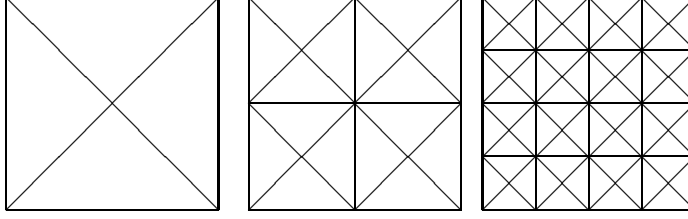


FIGURE 6.1. The first three levels of grids in all numerical tests.

TABLE 6.1. The error $e_h = I_h u - u_h$ and the order of convergence, by the P_2 conforming interpolated finite element and by the P_2 Lagrange finite element.

grid	$\ e_h\ _0$ h^n		$ e_h _1$ h^n		$\ e_h\ _0$ h^n		$ e_h _1$ h^n	
	P_2 Interpolated		conforming FE		P_2 Lagrange element			
4	0.614E-03	3.2	0.499E-01	2.0	0.615E-03	3.2	0.500E-01	2.0
5	0.723E-04	3.1	0.124E-01	2.0	0.723E-04	3.1	0.124E-01	2.0
6	0.887E-05	3.0	0.309E-02	2.0	0.887E-05	3.0	0.309E-02	2.0
7	0.110E-05	3.0	0.773E-03	2.0	0.110E-05	3.0	0.773E-03	2.0
8	0.138E-06	3.0	0.193E-03	2.0	0.138E-06	3.0	0.193E-03	2.0
9	0.172E-07	3.0	0.483E-04	2.0	0.172E-07	3.0	0.483E-04	2.0

TABLE 6.2. The error $e_h = I_h u - u_h$ and the order of convergence, by the P_2 interpolated nonconforming finite element and by the P_2 nonconforming finite element.

grid	$\ e_h\ _0$ h^n		$ e_h _1$ h^n		$\ e_h\ _0$ h^n		$ e_h _1$ h^n	
	P_2 Interpolated		nonconforming FE		P_2 nonconforming element			
2	0.503E-02	3.8	0.839E-01	2.3	0.124E-01	3.2	0.186E+00	2.5
3	0.118E-02	2.1	0.363E-01	1.2	0.164E-02	2.9	0.495E-01	1.9
4	0.181E-03	2.7	0.111E-01	1.7	0.208E-03	3.0	0.126E-01	2.0
5	0.244E-04	2.9	0.298E-02	1.9	0.260E-04	3.0	0.315E-02	2.0
6	0.316E-05	3.0	0.767E-03	2.0	0.325E-05	3.0	0.789E-03	2.0
7	0.406E-06	3.0	0.194E-03	2.0	0.407E-06	3.0	0.197E-03	2.0

In Table 6.3 we list the results of P_3 interpolated finite elements (4.2) and the P_3 Lagrange finite elements.

We then solve problem (1.2) by the $P_4/P_5/P_6$ interpolated finite element methods (4.7) and by the $P_4/P_5/P_6$ Lagrange finite element methods. The errors and the orders of convergence are listed in Table 6.4. The optimal order of convergence is achieved in all cases.

TABLE 6.3. The error $e_h = I_h u - u_h$ and the order of convergence, by the P_3 interpolated finite element and by the P_3 Lagrange finite element.

grid	$\ e_h\ _0$	h^n	$ e_h _1$	h^n	$\ e_h\ _0$	h^n	$ e_h _1$	h^n
	P_3 interpolated element				P_3 Lagrange element			
4	0.119E-04	4.0	0.114E-02	2.9	0.118E-04	4.0	0.114E-02	3.0
5	0.742E-06	4.0	0.143E-03	3.0	0.742E-06	4.0	0.143E-03	3.0
6	0.464E-07	4.0	0.180E-04	3.0	0.464E-07	4.0	0.180E-04	3.0
7	0.290E-08	4.0	0.225E-05	3.0	0.290E-08	4.0	0.225E-05	3.0
8	0.181E-09	4.0	0.281E-06	3.0	0.181E-09	4.0	0.281E-06	3.0

TABLE 6.4. The error $e_h = I_h u - u_h$ and the order of convergence, by the $P_4/P_5/P_6$ interpolated finite elements and by the $P_4/P_5/P_6$ Lagrange finite elements.

grid	$\ e_h\ _0$	h^n	$ e_h _1$	h^n	$\ e_h\ _0$	h^n	$ e_h _1$	h^n
	P_4 interpolated element				P_4 Lagrange element			
4	0.136E-06	4.7	0.132E-04	3.9	0.159E-06	5.0	0.142E-04	4.0
5	0.464E-08	4.9	0.859E-06	3.9	0.501E-08	5.0	0.891E-06	4.0
6	0.151E-09	4.9	0.547E-07	4.0	0.157E-09	5.0	0.557E-07	4.0
	P_5 interpolated element				P_5 Lagrange element			
3	0.484E-06	6.0	0.501E-04	4.9	0.478E-06	6.0	0.499E-04	4.9
4	0.755E-08	6.0	0.158E-05	5.0	0.754E-08	6.0	0.158E-05	5.0
5	0.118E-09	6.0	0.495E-07	5.0	0.118E-09	6.0	0.495E-07	5.0
	P_6 interpolated element				P_6 Lagrange element			
2	0.144E-05	6.6	0.639E-04	5.6	0.336E-06	7.2	0.164E-04	6.3
3	0.122E-07	6.9	0.102E-05	6.0	0.276E-08	6.9	0.259E-06	6.0
4	0.972E-10	7.0	0.160E-07	6.0	0.218E-10	7.0	0.406E-08	6.0

REFERENCES

- [1] P. Alfeld, and T. Sorokina, Linear Differential Operators on Bivariate Spline Spaces and Spline Vector Fields, BIT Numerical Mathematics, 56(1), 15-32, 2016.
- [2] D. N. Arnold, D. Boffi and R. S. Falk, Approximation by quadrilateral finite elements. Math. Comp. 71 (2002), no. 239, 909-922.
- [3] J. H. Bramble and S. R. Hilbert, Estimation of linear functionals on Sobolev spaces with applications to Fourier transforms and spline interpolation, SIAM J. Numer. Anal., 7 (1970), 113–124.
- [4] S. C. Brenner and L. R. Scott, The mathematical theory of finite element methods. Third edition. Texts in Applied Mathematics, 15. Springer, New York, 2008.
- [5] R. S. Falk, P. Gatto and P. Monk, Hexahedral H(div) and H(curl) finite elements. ESAIM Math. Model. Numer. Anal. 45 (2011), no. 1, 115-143.
- [6] J. Hu, Y. Huang and S. Zhang, The lowest order differentiable finite element on rectangular grids, SIAM Num. Anal. 49 (2011), No 4, 1350–1368.
- [7] J. Hu and S. Zhang, The minimal conforming H^k finite element spaces on R^n rectangular grids, Math. Comp. 84 (2015), no. 292, 563–579.
- [8] J. Hu and S. Zhang, Finite element approximations of symmetric tensors on simplicial grids in R^n : the lower order case, Math. Models Methods Appl. Sci. 26 (2016), no. 9, 1649–1669.
- [9] Y. Huang and S. Zhang, Supercloseness of the divergence-free finite element solutions on rectangular grids, Commun. Math. Stat. 1 (2013), no. 2, 143–162.
- [10] M.-J. Lai and L. L. Schumaker, Spline functions on triangulations, Cambridge University Press, Cambridge, 2007.
- [11] M. Li, S. Mao and S. Zhang, New error estimates of nonconforming mixed finite element methods for the Stokes problem, Math. Methods Appl. Sci. 37 (2014), no. 7, 937–951.
- [12] L. L. Schumaker, T. Sorokina and A. J. Worsey, A C1 quadratic trivariate macro-element space defined over arbitrary tetrahedral partitions. J. Approx. Theory, 158 (2009), No. 1, 126–142.
- [13] L.R. Scott and S. Zhang, Finite element interpolation of nonsmooth functions satisfying boundary conditions, Math. Comp. 54 (1990), 483–493.
- [14] T. Sorokina and S. Zhang, Conforming harmonic finite elements on the Hsieh-Clough-Tocher split of a triangle, Int. J. Numer. Anal. Model., 17 (2020) no. 1, 54–67.
- [15] T. Sorokina and S. Zhang, Conforming and nonconforming harmonic finite elements, Applicable Analysis, Appl. Anal. 99 (2020), no. 4, 569–584.
- [16] C. Wang, S. Zhang, Shangyou and J. Chen, A unified mortar condition for nonconforming finite elements, J. Sci. Comput. 62 (2015), no. 1, 179–197.
- [17] M. Zhang and S. Zhang, A 3D conforming-nonconforming mixed finite element for solving symmetric stress Stokes equations, Int. J. Numer. Anal. Model. 14 (2017), no. 4-5, 730–743.
- [18] S. Zhang, A C1-P2 finite element without nodal basis, M2AN 42 (2008), 175–192.
- [19] S. Zhang, A family of 3D continuously differentiable finite elements on tetrahedral grids, Applied Numerical Mathematics, 59 (2009), no. 1, 219–233.
- [20] S. Zhang, A family of differentiable finite elements on simplicial grids in four space dimensions, (Chinese) Math. Numer. Sin. 38 (2016), no. 3, 309–324.
- [21] S. Zhang, Coefficient jump-independent approximation of the conforming and nonconforming finite element solutions, Adv. Appl. Math. Mech. 8 (2016), no. 5, 722–736.
- [22] S. Zhang, A P4 bubble enriched P3 divergence-free finite element on triangular grids, Comput. Math. Appl. 74 (2017), no. 11, 2710–2722.

DEPARTMENT OF MATHEMATICS, TOWSON UNIVERSITY, 7800 YORK ROAD, TOWSON, MD 21252, USA. TSOROKINA@TOWSON.EDU

DEPARTMENT OF MATHEMATICAL SCIENCES, UNIVERSITY OF DELAWARE, NEWARK, DE 19716, USA. SZHANG@UDEL.EDU